

# Analysis of Black Carbon Concentrations in PM<sub>2.5-10</sub> and PM<sub>2.5</sub> Fractions by MABI Instrument in Two Urban Areas of Dakar, Senegal

Alassane Traore<sup>1,\*</sup>, Moustapha Kebe<sup>1</sup>, Malick Sow<sup>1</sup>, Vasiliki Vasilatou<sup>2</sup>, Ababacar Sadikhe Ndao<sup>1</sup>, Konstantinos Eleftheriadis<sup>2</sup>

<sup>1</sup>Faculty des Sciences et Techniques, University Cheikh Anta Diop Dakar, Dakar, Senegal

<sup>2</sup>Environmental Radioactivity & Aerosol technology for Atmospheric and Climate Impact N. C. S. R. Demokritos, Agia Paraskevi, Attiki, Greece

## Email address:

alassane2.traore@ucad.edu.sn (Alassane Traore), moustapha5.kebe@ucad.edu.sn (Moustapha Kebe),

malick711.sow@ucad.edu.sn (Malick Sow), vasiliki@ipta.demokritos.gr (Vasiliki Vasilatou),

ababacar.ndao@ucad.edu.sn (Ababacar Sadikhe Ndao), elefther@ipta.demokritos.gr (Konstantinos Eleftheriadis)

\*Corresponding author

## To cite this article:

Alassane Traore, Moustapha Kebe, Malick Sow, Vasiliki Vasilatou, Ababacar Sadikhe Ndao, Konstantinos Eleftheriadis. Analysis of Black Carbon Concentrations in PM<sub>2.5-10</sub> and PM<sub>2.5</sub> Fractions by MABI Instrument in Two Urban Areas of Dakar, Senegal. *International Journal of Atmospheric and Oceanic Sciences*. Vol. 7, No. 2, 2023, pp. 23-30. doi: 10.11648/j.ijaos.20230702.11

Received: August 29, 2023; Accepted: September 19, 2023; Published: October 8, 2023

**Abstract:** Black carbon (BC) is a particular pollutant that absorbs visible light and can intervene in the climatic change with irradiance. The sources of BC emissions are known, such as incomplete combustion of fossil fuels and biomass burning. Our study focuses on two sites Hlm and Yoff in Dakar, Senegal in order to determine the mass absorption coefficient of BC in our polycarbonate nucleopore filters from November 2018 to October 2019 so as to collect PM<sub>2.5</sub> and PM<sub>2.5-10</sub> we face in our two study sites using MABI instrument. In addition, we investigate the source apportionment of black carbon in PM<sub>2.5</sub> fraction. We observe that the mass absorption coefficient of PM<sub>2.5</sub> is higher than that of PM<sub>2.5-10</sub>. The average concentration of BC at Hlm and Yoff were  $1.85 \pm 0.37$  and  $2.69 \pm 0.54 \mu\text{g}\cdot\text{m}^{-3}$  respectively, whereas the average concentrations of BC<sub>BB</sub> were  $0.003 \pm 0.0007$  and  $0.08 \pm 0.01 \mu\text{g}\cdot\text{m}^{-3}$ , respectively and for BC<sub>FF</sub> were  $1.85 \pm 0.37$  and  $2.61 \pm 0.53 \mu\text{g}\cdot\text{m}^{-3}$ . The BC from at Yoff has two compounds with 2.97% of Biomass burning and 97, 03% of Fossil fuels in contrast to Hlm site the black carbon was mainly composed of fossil fuels in Dakar, the fossil fuels are mainly source of the black carbon.

**Keywords:** BC, BC<sub>FF</sub>, BC<sub>BB</sub>, PM, MABI

## 1. Introduction

Air pollution has always been a topic of interest for researchers because of its adverse effects on health, the environment and the climate [1-4] Today, thanks to the research conducted on air pollution, we have become aware of the pollutants present in the air, namely heavy metals, chemical elements, organic and inorganic substances and particulate matters (PM). Particle matters have different aerodynamic diameters. In addition, we have elemental carbon (EC) and organic carbon (OC) which form carbonaceous aerosols and which are among the components

of particle matters (PM).

Carbonaceous species, organic carbon (OC) and black carbon (BC) constitute a significant portion of fine particles [5]. Sources of BC emissions are known, such as incomplete combustion of fossil fuels and biomass burning [6, 7]. BC absorbs all wavelengths of solar radiation [8] and is considered one of the contributors to global warming in terms of direct impact [9, 10]. Organic carbon is adjective, but is responsible for the appearance of a brown haze and reduced visibility at a site [11]. Research on OC has been very fruitful in terms of the composition of the optical properties and morphology of the particle, so that it has been given several names in terminology. In the literature it is sometimes referred

to as "black carbon", for example: "soot", "light absorbing carbon", "elemental carbon", "refractory carbon", "graphitic carbon" has been used as terminologies [12].

In many studies on BC, several techniques for analysis and determination of its mass concentration have been used in urban and semi-rural areas [13-15] to determine the distribution of BC sources [16-19]. Some commonly used techniques are: the smoke stain reflectometer (such as an EEL (Evans Electro selenium 78 Ltd)) [20], Aethalometer (AE33) [21].

Dakar, the capital of Senegal, is the most developed city in the country, with a population of 5 million. There are many industrial activities in Dakar such as agri-food, automotive, wood and paper, plastics, textiles, oil and construction... We should also notice here there is an interesting agricultural sector in Dakar. In fact, it has been noticed a rapid increase in the number of cars and black carbon emissions. This has as result the change of the environment in Dakar. This is the reason why there is interest in a first study on BC sources in Dakar.

The objectives of this study were to determine the mass absorption coefficient of BC in our polycarbonate nucleopore filters during the period of our sampling campaign to collect PM<sub>2.5</sub> and PM<sub>2.5-10</sub> present in our two study sites namely Hlm an industrial location and Yoff, a coastal location. Measure the equivalent concentration of BC in each PM<sub>2.5</sub> filter, make the distribution of the BC sources contained in the PM<sub>2.5</sub> filters and last point, observe the temporal evolution between BC from incomplete biomass combustion and BC from fossil fuel combustion at the two sites studied.

## 2. Experiments

### 2.1. Sampling Sites

The measurement campaigns were carried out at two different urban sites (Hlm and Yoff) in Senegal. Particulate matters sampling was conducted using a low-volume sampler from the University of GENT, which collected PM<sub>2.5</sub> and PM<sub>2.5-10</sub> samples from the Hlm and Yoff sites. The measurement period was from November 2018 to October 2019. Samples of PM<sub>2.5-10</sub> and PM<sub>2.5</sub> were taken twice during a week (one business day and one weekend) at each site. Sampling, elemental sample analysis, and source distribution of the collected particulate matters (PM) were described by Kebe *et al.* [22].

### 2.2. Multi-Wavelength Absorption Black Carbon Instrument for Black Carbon Analysis

The samples were analyzed for Black Carbon by Multi-Wavelength Absorption Black Carbon (MABI). MABI was developed by ANSTO. It measures absorption light through unexposed filters (I<sub>0</sub>) and (I) exposed to sample particles at seven different fixed wavelengths: 405 nm, 465 nm, 525 nm, 639 nm, 870 nm, 940 nm, and 1050 nm. To disperse the light scattered through the filter towards the detector, the filter must face the detector and not the light

source in our MABI unit [23]. Knowing the values (I<sub>0</sub>) and (I), the surface of the exposed area of the filters (A) and sampled air volume (V) for each 47mm nucleopore polycarbonate filter used, we can first calculate the light absorption coefficient  $b_{abs}$  (M.m<sup>-1</sup>) according to the following equation:

$$b_{abs} = 10^2 * \frac{A}{V} \ln * \left[ \frac{I_0}{I} \right] \quad (1)$$

A = Filter collection area in cm<sup>2</sup>

V = Volume of air sampled through the filter in m<sup>3</sup>

I<sub>0</sub> = Measured light transmission and reflection through blank (unexposed) filter

I = Measured light transmission and reflection through filter after particle sampling.

The black carbon (BC) mass concentration (ng.m<sup>-3</sup>) was determined using a mass absorption coefficient  $\epsilon$  (m<sup>2</sup>.g<sup>-1</sup>) at each wavelength according the following equation:

$$BC = 10^5 * \frac{A}{\epsilon * V} \ln * \left[ \frac{I_0}{I} \right] \quad (2)$$

The values of the mass absorption coefficient  $\epsilon$  vary between 4-9 m<sup>2</sup>.g<sup>-1</sup> for PM<sub>2.5</sub> and 1 to 2 m<sup>2</sup>.g<sup>-1</sup> for PM<sub>2.5-10</sub> [24].

The variability of the mass absorption coefficient with  $\epsilon$  wavelength is [25, 26]:

$$\epsilon(\lambda) = a. \lambda^{-\alpha} \quad (3)$$

## 3. Results

### 3.1. Measurements

To determine the mass absorption coefficient  $\epsilon(\lambda)$  for each wavelength, the first step is to use the wavelength  $\lambda_1 = 639 \text{ nm}$  and assume  $\epsilon(\lambda_1) = 6.599 \text{ m}^2.\text{g}^{-1}$  and  $1.206 \text{ m}^2.\text{g}^{-1}$  for PM<sub>2.5</sub> and PM<sub>2.5-10</sub> respectively which were provided by the manufacturer for the 47 mm diameter nucleopore polycarbonate filters, at the last we plot  $\ln(I_0/I)$  for each wavelength  $\lambda$  against  $\ln(I_0/I)$  of the wavelength  $\lambda_1 = 639 \text{ nm}$  and multiplying the gradient of these plots by the mass absorption coefficient  $\epsilon(\lambda_1)$ .

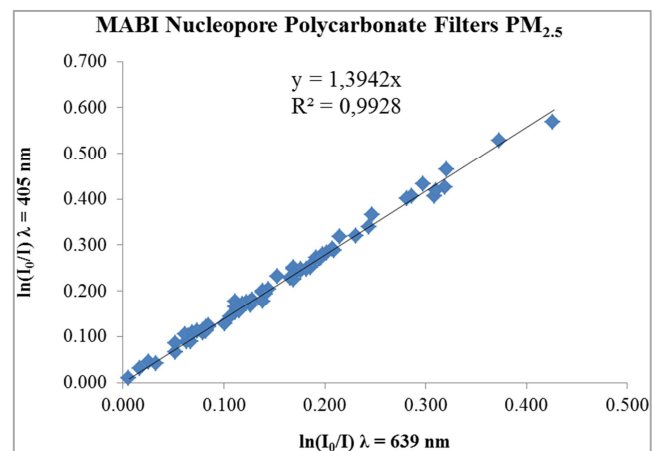


Figure 1. The  $\ln(I_0/I)$  plot for  $\lambda=405\text{nm}$  against  $\ln(I_0/I)$  for  $\lambda=639\text{nm}$  for over 70 filters PM<sub>2.5</sub> from Hlm and Yoff sampling sites in Dakar between November 2018 and November 2019.

Figure 1 shows that the adjusted coefficient called gradient is equal to 1.3942 and a correlation coefficient  $R^2 = 0.9928$ . Using equation (3) we obtain the mass absorption coefficients  $\epsilon(\lambda_{405nm})$  equals to  $9.21 \text{ m}^2 \cdot \text{g}^{-1}$  for the  $\text{PM}_{2.5}$  collected at Hlm and Yoff sites. Thus, to know the mass absorption coefficient  $\epsilon(\lambda)$  of each wavelength of the MABI instrument this process is repeated, always maintaining  $\epsilon(\lambda_1)$ .

In addition, we want to determine the mass absorption coefficient of  $\text{PM}_{2.5-10}$  by plotting  $\ln(I_0/I)$  plot for  $\lambda=1050\text{nm}$  against  $\ln(I_0/I)$  for  $\lambda=639\text{nm}$  while remaining in the same Hlm and Yoff sites with the same number of samples as  $\text{PM}_{2.5}$  in figure 1.

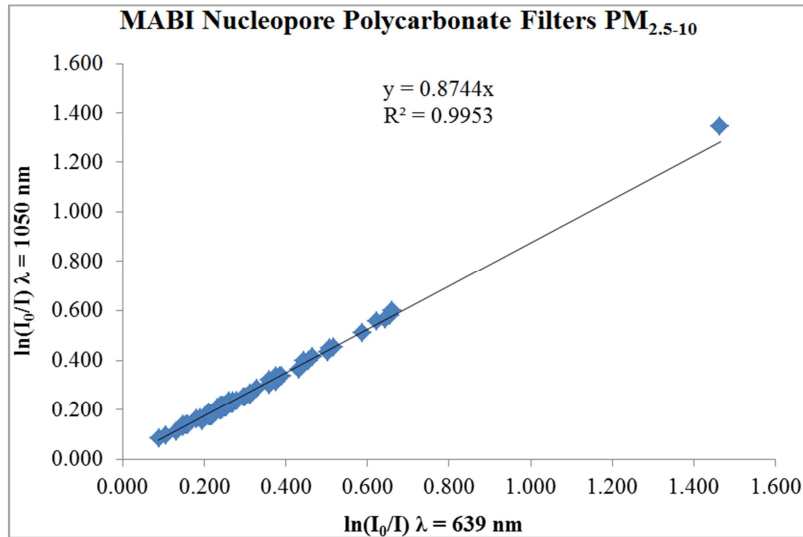


Figure 2. The  $\ln(I_0/I)$  plot for  $\lambda=1050\text{nm}$  against  $\ln(I_0/I)$  for  $\lambda=639\text{nm}$  for over 70 filters  $\text{PM}_{2.5-10}$  from Hlm and Yoff sampling sites in Dakar between November 2018 and October 2019.

Figure 2 shows that the adjusted coefficient called gradient is equal to 0.8744 and a correlation coefficient  $R^2 = 0.9953$ . We obtain the mass absorption coefficients  $\epsilon(\lambda_{1050nm})$  equals to  $1.054 \text{ m}^2 \cdot \text{g}^{-1}$  for the  $\text{PM}_{2.5-10}$  collected at Hlm and Yoff sites.

In the same way as in Figures 1 and 2, we determine the variation of the mass absorption coefficient as a function of the seven wavelengths of the MABI instrument.

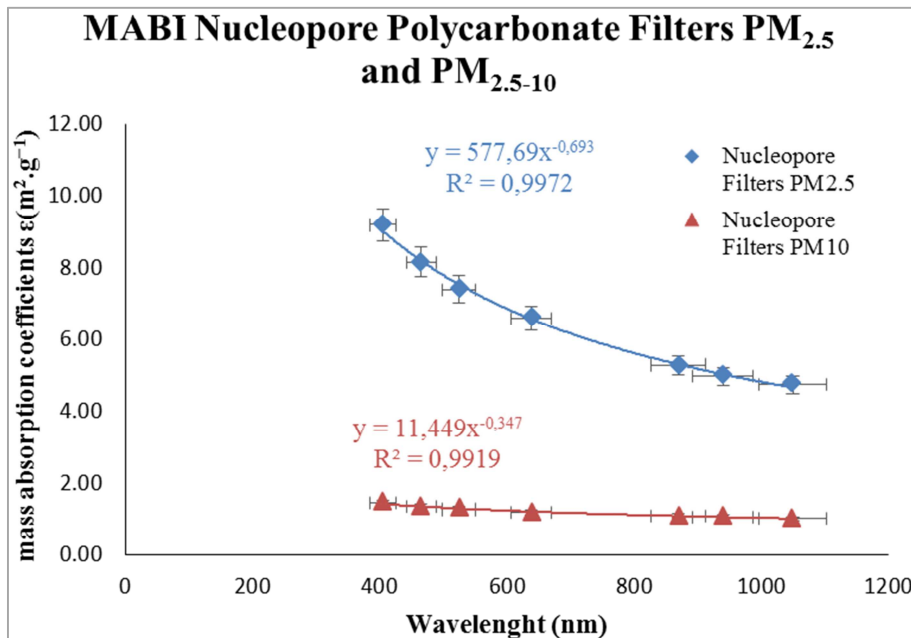


Figure 3. Variation of the mass absorption coefficient as a function of wavelength for  $\text{PM}_{2.5}$  and  $\text{PM}_{2.5-10}$  from Hlm and Yoff sampling sites.

Figure 3 shows the variations of the mass absorption coefficient  $\epsilon(\lambda)$  with wavelength (nm) for 47 mm exposed Nucleopore polycarbonate filters  $\text{PM}_{2.5}$  and  $\text{PM}_{2.5-10}$  from Hlm

and Yoff sampling sites. The powerful law (Theory of Mie) gives the mass absorption coefficient adjusted with with a = 577.69,  $\alpha = 0.693$  and an excellent correlation coefficient  $R^2$

= 0.9972 for the PM<sub>2.5</sub> and for the PM<sub>2.5-10</sub> we obtain a = 11.449,  $\alpha = 0.347$  and correlation coefficient R<sup>2</sup> equals to 0.9919. We observe that the mass absorption coefficient of PM<sub>2.5</sub> is higher than that of PM<sub>2.5-10</sub>. The exponent  $\alpha$  called Angstrom exponent [27] in generally can be accepted around unity for BC from high temperature fossil fuel combustion [28]. Ours values  $\alpha$  are fall within 0.4 <  $\alpha$  < 1 as indicated [23] using MABI systems.

### 3.2. Determination of Black Carbon Concentrations

To determine equivalent BC concentrations (eBC) with the MABI instrument we used Equation (2) with a mass absorption coefficient  $\epsilon(\lambda_{639nm})$  equals to 6.60 m<sup>2</sup>.g<sup>-1</sup> as recommended in manual MABI.

The Black Carbon concentrations found in PM<sub>2.5</sub> fraction in Hlm and Yoff sites are presented in Table 1:

**Table 1.** Equivalent BC concentrations of the collected PM<sub>2.5</sub> from November 2018 to October 2019 in  $\mu\text{g}\cdot\text{m}^{-3}$ .

	Hlm	Yoff
Mean	1.85 ± 0.37	2.69 ± 0.54
Median	1.6 ± 0.32	2.68 ± 0.54
Maximum	6.84 ± 1.37	4.98 ± 0.99
Minimum	0.1 ± 0.019	0.28 ± 0.06

The mean value for eBC concentrations at Hlm is 1.85  $\mu\text{g}\cdot\text{m}^{-3}$  and and 2.69  $\mu\text{g}\cdot\text{m}^{-3}$  at Yoff. The mean value concentration of eBC is more relevant in Yoff than in Hlm. The traffic related emissions contribute more than industrial activities in Dakar. This fact is a possible hypothesis due to the BC from fossil fuel combustion is more prevalent than the one from biomass combustion at the Yoff and Hlm sites. In this study, the mean values of eBC at Hlm and Yoff were similar to Italy [29], India [30] and Nanjing [31] respectively.

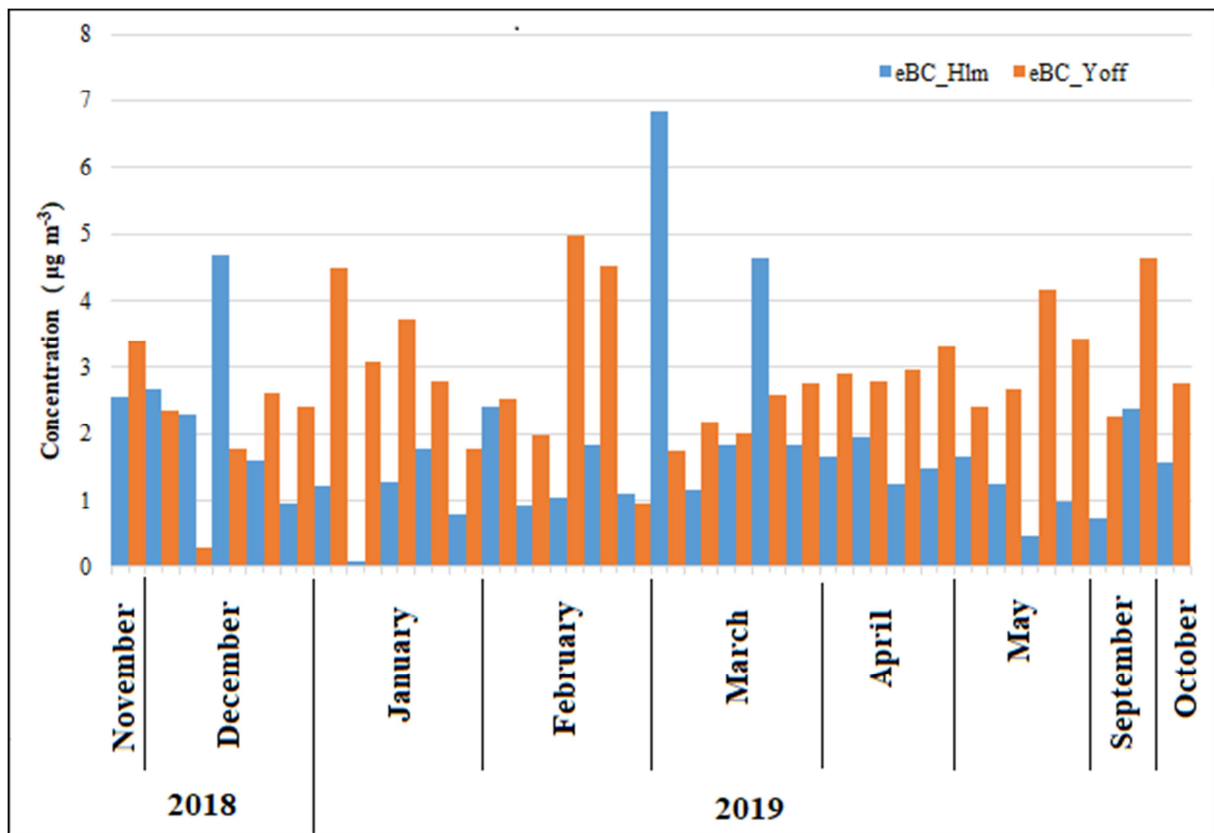


**Figure 4.** Comparison daily eBC concentrations for 639 nm at Hlm and Yoff sites from November 2018 to October 2019 in  $\mu\text{g}\cdot\text{m}^{-3}$ .

Figure 4 shows the variation of daily eBC concentrations with wavelength 639 nm at the two sites from November 2018 to October 2019 in  $\mu\text{g}\cdot\text{m}^{-3}$ . In Figure 4, the blue vertical bar is the equivalent black carbon concentration at the Hlm site and the orange vertical bar is the equivalent black carbon concentration at the Yoff site. We have higher eBC concentrations at Hlm than Yoff only for a few days in December 2018 and March 2019. This can be explained by assuming that all plants were operating at that time. Previously, we know that industrial emissions and road traffic were sources of pollution at the Yoff and Hlm sites revealed in our previous study.

### 3.3. Source Apportionment of BC at Hlm and Yoff Sites

Black carbon (BC) particles come primarily from two sources: combustion of high temperature fossil fuels and combustion of low temperature biomass. By subtracting the BC data (1050 nm) from the BC data (450 nm), the BC from biomass combustion is obtained primarily. Black carbon particles formed at high temperatures are typically small, 100-300 nm in diameter, solid and spherical [32]. Carbon black from high temperature combustion absorbs more in infrared, while the low temperature absorbs at shorter

wavelengths (U. V) [33]. The mean values and standard deviations of the concentrations  $BC_{bb}$  and  $BC_{ff}$  in Hlm and

Yoff cities are in Table 2.

**Table 2.** Summary of the mean value, median, maximum (max) and minimum concentrations of  $BC_{FF}$  (fossil-fuel BC) and  $BC_{BB}$ , (biomass burning BC), Hlm and Yoff sites from November 2018 to October 2019 in  $\mu\text{g.m}^{-3}$ .

	Hlm		Yoff	
	$BC_{BB}$	$BC_{FF}$	$BC_{BB}$	$BC_{FF}$
Mean	$0.003 \pm 0.0007$	$1.85 \pm 0.37$	$0.08 \pm 0.01$	$2.61 \pm 0.53$
Median	$0.03 \pm 0.005$	$1.63 \pm 0.33$	$0.08 \pm 0.01$	$2.6 \pm 0.52$
Maximum	$0.48 \pm 0.1$	$6.36 \pm 1.28$	$0.45 \pm 0.09$	$4.53 \pm 0.91$
Minimum	$-0.46 \pm -0.1$	$0.56 \pm 0.12$	$-0.25 \pm -0.05$	$0.53 \pm 0.10$

Biomass burning ( $BC_{BB}$ ) and fossil fuels ( $BC_{FF}$ ) mean values were  $0.003 \pm 0.0007 \mu\text{g m}^{-3}$  and  $1.85 \pm 0.37 \mu\text{g.m}^{-3}$  at Hlm site,  $0.08 \pm 0.01 \mu\text{g.m}^{-3}$  and  $2.61 \pm 0.53 \mu\text{g.m}^{-3}$  at Yoff site respectively.  $BC_{BB}$  values can be negative but we expect its mean value to be zero and defined as a smoke diesel between  $\pm 0.05 \mu\text{g.m}^{-3}$  [23]. From Hlm site it was expected the average value of  $BC_{BB}$  equals to zero because this location has characteristic industrial and there are no significant biomass burning event during the sampling period. The pollution come from traffic emission and fossil fuels combustion. Whereas at Yoff site mean percentage of biomass burning (%BB) was  $2.97 \pm 0.6$ . Fossil fuel burning activities are most predominant than biomass burning activities in Yoff. The source apportionment shows that BC are mainly emitted from fossil-fuel sources in Hlm site whereas a mean percentage of fossil fuels (%FF) equals to  $97.03\% \pm 19.41$  at Yoff site.

The determination for the fossil fuels concentrations at Hlm and Yoff sites was obtained by the following equation:

$$BC = BC_{BB} + BC_{FF} \quad (4)$$

Figures 5 and 6 show the distribution of BC (blue line),  $BC_{BB}$  (red line) and  $BC_{FF}$  (purple line) levels in Dakar using equation (6).

Figure 5 shows that BC ranges between  $0.1 \pm 0.019 \mu\text{g.m}^{-3}$  and  $6.84 \pm 1.37 \mu\text{g.m}^{-3}$ . The figure includes at both the variations of  $BC_{BB}$  and  $BC_{FF}$  concentrations over time. The maximum and minimum values  $BC_{BB}$  and  $BC_{FF}$  were  $0.48 \pm 0.1 \mu\text{g.m}^{-3}$  and  $0.46 \pm 0.1 \mu\text{g.m}^{-3}$ ;  $6.36 \pm 1.28 \mu\text{g.m}^{-3}$ ; and  $0.56 \pm 0.12 \mu\text{g.m}^{-3}$  respectively. The negative value  $BC_{BB}$  is the fact we have the presence of diesel smoke at Hlm indeed it is an industrial area in addition to this, there is road traffic. The peaks of  $BC_{FF}$  above the equivalent BC concentration for some days in the Figure 5 are explained by the fact that the value for  $BC_{BB}$  was negative. We can conclude that the  $BC_{FF}$  concentrations are equal generally those BC concentrations at Hlm site.

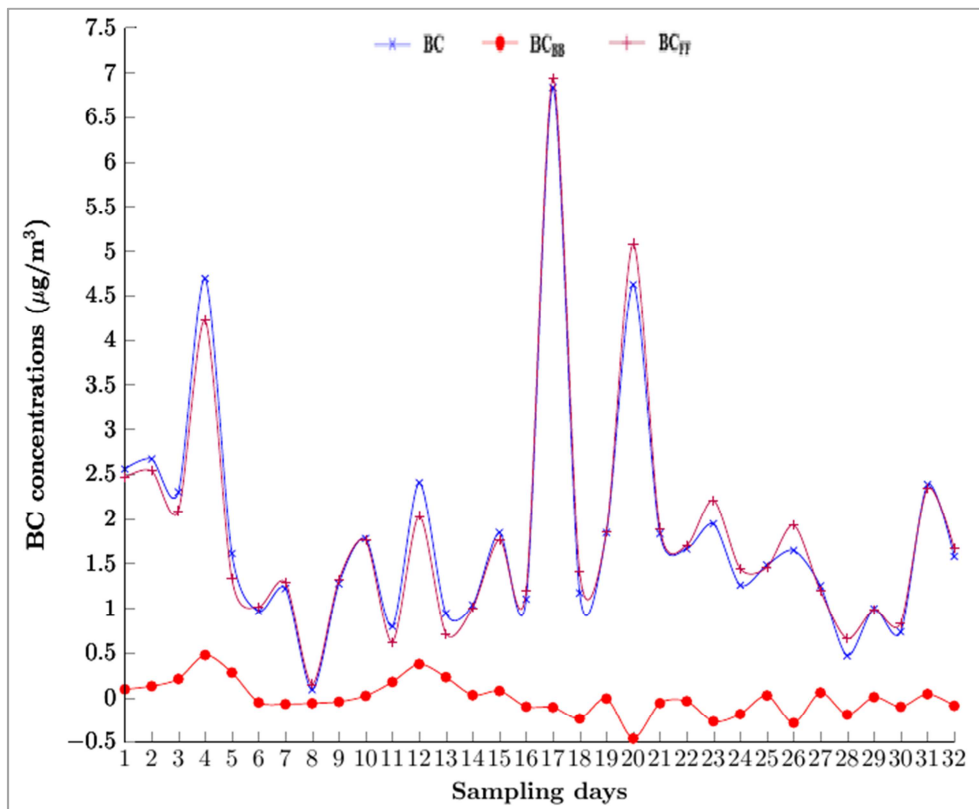


**Figure 5.** Evolution of BC,  $BC_{BB}$  and  $BC_{FF}$  concentrations over time at Hlm site.

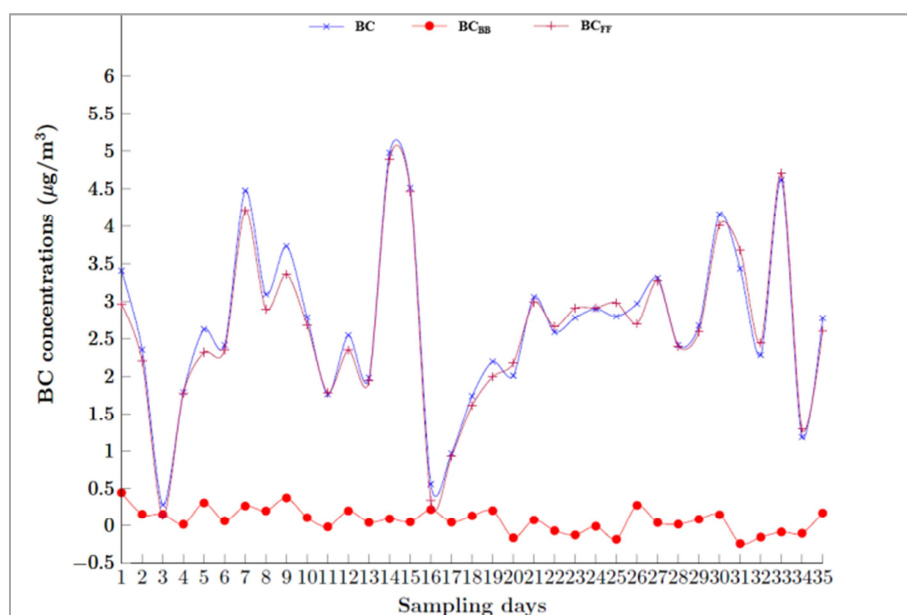


Figure 6. Evolution of BC, BC<sub>BB</sub> and BC<sub>FF</sub> concentrations with time at Yoff site.

In Figure 6, BC ranges between  $0.28 \pm 0.06 \mu\text{g.m}^{-3}$  and  $4.98 \pm 0.99 \mu\text{g.m}^{-3}$  whereas the variations of BC<sub>BB</sub> concentrations with time were between the range  $0.25 \pm 0.05 \mu\text{g.m}^{-3}$  and  $0.45 \pm 0.09 \mu\text{g.m}^{-3}$ ; and for BC<sub>FF</sub> we have  $0.53 \pm 0.10 \mu\text{g.m}^{-3}$  to  $4.53 \pm 0.91 \mu\text{g.m}^{-3}$ . The black carbon from biomass burning at Yoff site is higher than Hlm site, with a percent of 2.97%.

#### 4. Conclusion

The black carbon concentrations were determined by MABI instrument. The average concentration of BC at Hlm and Yoff were  $1.85 \pm 0.37$  and  $2.69 \pm 0.54 \mu\text{g.m}^{-3}$  respectively, whereas the average concentrations of BC<sub>BB</sub> were  $0.003 \pm 0.0007$  and  $0.08 \pm 0.01 \mu\text{g.m}^{-3}$ , respectively and for BC<sub>FF</sub> were  $1.85 \pm 0.37$  and  $2.61 \pm 0.53 \mu\text{g.m}^{-3}$ . The BC from at Yoff has two compounds with 2.97% of Biomass burning and 97, 03% of Fossil fuels in contrast to Hlm site the black carbon was mainly composed of fossil fuels in Dakar, the fossil fuels are principally source of the black carbon.

The information obtained from this study has provided us with knowledge on the sources of BC and we will be able to restrict the number of diesel vehicles and reduce BC emissions from anthropogenic activities.

#### Authors Contributions

Conceptualization, A. T. and M. K.; methodology, A. T. and M. K.; validation, M. K. and A. T.; formal analysis, M. K. A. T. and V. V.; writing—original draft preparation, M. K. and A. T.; writing—review and editing, A. T. and M. K.; supervision, A. T.; Administrative issue, A. S. N. All authors have read and agreed to the published version of the manuscript.

#### Conflict of Interest

The authors declare that the research was conducted in the absence of any commercial or financial relationships that could be construed as a potential conflict of interest.

#### Funding

This research was funded by the International Atomic Energy Agency in Vienna under the framework of the Regional technical project RAF7016.

#### Acknowledgments

We are very grateful to Roman Padilla Alvarez for his support during the entire duration of the project, the sampling protocol and advice.

#### References

- [1] Elichegaray, C. (2001). Département Air à l'Agence de l'environnement et de la maîtrise de l'énergie (ADEME). Pollut. Atmosphérique.
- [2] Li, W.; Bai, Z.; Liu, A.; Chen, J.; Chen, I. (2009). Characteristics for major PM<sub>2.5</sub> components during winter in Tianjin, China. *Aerosol Air Qual. Res.*, 9, 105–119. [CrossRef].
- [3] Katsouyanni, K.; Touloumi, G.; Samoli, E.; Gryparis, A.; Le Tertre, A.; Monopoli, Y.; Rossi, G.; Zmirou, D.; Ballester, F.; Boumghar, A.; et al. (2001). Confounding and effect modification in the short-term effects of ambient particles on total mortality: Results from 29 European cities within the APHEA2 Project. *Epidemiology*, 12, 521–531. [CrossRef] [PubMed].

- [4] Liu, Y.; Daum, P. H. (2002). Anthropogenic aerosols: Indirect warming effect from dispersion forcing. *Nature*, 419, 580–581. [CrossRef].
- [5] Begum, B. A., Hossain, A., Nahar, N., Markwitz, A., Hopke, P. K. (2012). Organic and Black Carbon in PM<sub>2.5</sub> at an Urban Site at Dhaka, Bangladesh. *Aerosol and Air Quality Research*, 12: 1062-1072.
- [6] Mayol-Bracero, O., Gabriel, R., Andreae, M., Kirchstetter, T., Novakov, T., Ogren, J., Sheridan, P., and Streets, D., (2007). Carbonaceous Aerosols over the Indian Ocean during the Indian Ocean Experiment (INDOEX): Chemical Characterization, Optical Properties, and Probable Sources. *J. Geophysics Research*. 107: 8030.
- [7] Bond, T. C., (2007). Can Warming Particles Enter Global Climate Discussions? *Environmental Research Letter* 2, pp 208.
- [8] Bond, T. C. and Bergstrom, R. W. 2006: Light Absorption by Carbonaceous Particles: An Investigative Review, *Aerosol Sci. Technol.*, 40 (1), 27–67, <https://doi.org/10.1080/02786820500421521>,
- [9] Jacobson, M. Z. (2001): Strong radiative heating due to the mixing state of black carbon in atmospheric aerosols, *Nature*, 409 (6821), 695–697, <https://doi.org/10.1038/35055518>,
- [10] Liu, Q., Ma, T., Olson, M. R., Liu, Y., Zhang, T., Wu, Y. and Schauer, J. J. 2016: Temporal variations of black carbon during haze and non-haze days in Beijing, *Sci.Rep.*, 6 (1), 33331, <https://doi.org/10.1038/srep33331>.
- [11] Horvath, H. (1993): Atmospheric light absorption—A review, *Atmos. Environ. Part A. Gen. Top.*, 27 (3), 293–317, [https://doi.org/https://doi.org/10.1016/0960-1686\(93\)90104-7](https://doi.org/https://doi.org/10.1016/0960-1686(93)90104-7).
- [12] Petzold, A., Ogren, J. A., Fiebig, M., Laj, P., Li, S. M., Baltensperger, U., Holzer-Popp, T., Kinne, S., Pappalardo, G., Sugimoto, N., Wehrli, C., Wiedensohler, A. and Zhang, X. Y. 2013: Recommendations for reporting black carbon measurements, *Atmos. Chem. Phys.*, 13 (16), 8365–8379, <https://doi.org/10.5194/acp-13-8365-2013>
- [13] Yan, B.; Kennedy, D.; Miller, R. L.; Cowin, J. P.; Jung, K.-h.; Perzanowski, M.; Balletta, M.; Perera, F. P.; Kinney, P. L.; Chillrud, S. N. (2011). Validating a nondestructive optical method for apportioning colored particulate matter into black carbon and additional components. *Atmos. Environ.* 45, 7478–7486. [CrossRef].
- [14] Sharma, S.; Brook, J. R.; Cachier, H.; Chow, J.; Gaudenzi, A.; Lu, G. (2002). Light absorption and thermal measurements of black carbon in different regions of Canada. *J. Geophys. Res. Atmos.* 107, AAC 11-1–AAC 11-11. [CrossRef].
- [15] Ran, L.; Deng, Z. Z.; Wang, P. C.; Xia, X. A. (2016). Black carbon and wavelength-dependent aerosol absorption in the North China Plain based on two-year aethalometer measurements. *Atmos. Environ.* 142, 132–144. [CrossRef].
- [16] Sandradewi, J., Prévôt, A. S. H., Weingartner, E., Schmidhauser, R., Gysel, M., Baltensperger, U., (2008). A study of wood burning and traffic aerosols in an Alpine valley using a multi wavelength Aethalometer. *Atmos. Environ.* 42, 101–112.
- [17] Herich, H., Hueglin, C., Buchmann, B., (2011). A 2.5 year's source apportionment study of black carbon from wood burning and fossil fuel combustion at urban and rural sites in Switzerland. *Atmos. Meas. Tech.* 4, 1409–1420.
- [18] Zotter, P., Herich, H., Gysel, M., El-Haddad, I., Zhang, Y., Močnik, G., Hüglin, C., Baltensperger, U., Szidat, S., Prévôt, A. S., (2017). Evaluation of the absorption Ångström exponents for traffic and wood burning in the Aethalometer-based source apportionment using radiocarbon measurements of ambient aerosol. *Atmos. Chem. Phys.* 17, 4229–4249.
- [19] Healy, R., Sofowote, U., Su, Y., Deboasz, J., Noble, M., Jeong, C.-H., Wang, J., Hilker, N., Evans, G., Doerksen, G., (2017). Ambient measurements and source apportionment of fossil fuel and biomass burning black carbon in Ontario. *Atmos. Environ.* 161, 34–47.
- [20] Davy, P. M., Tremper, A. H., Nicolosi, E. M., Quincey, P., Fuller, G. W. J. A. E. (2017). Estimating particulate black carbon concentrations using two offline light absorption methods applied to four types of filter media, *Atmospheric Environment* 152, pp. 24-33.
- [21] Ezani, E.; Dhandapani, S.; Heal, M. R.; Praveena, S. M.; Khan, M. F.; Ramly, Z. T. A. (2021). Characteristics and Source Apportionment of Black Carbon (BC) in a Suburban Area of Klang Valley, Malaysia. *Atmosphere*, 12, 784. <https://doi.org/10.3390/atmos12060784>.
- [22] Kebe, M.; Traore, A.; Manousakas, M. I.; Vasilatou, V.; Ndao, A. S.; Wague, A.; Eleftheriadis, K. (2021). Source Apportionment and Assessment of Air Quality Index of PM<sub>2.5–10</sub> and PM<sub>2.5</sub> in at Two Different Sites in Urban Background Area in Senegal. *Atmosphere*, 12, 182. <https://doi.org/10.3390/atmos12020182>
- [23] David D. Cohen (2020): Summary of Light Absorbing Carbon and Visibility Measurements and Terms. ANSTO External Report ER- 790, ISBN – 1 921268 32 8.
- [24] Manohar, M., Atanacio, A., Button, D., Cohen, D., (2021). MABI - A multi-wavelength absorption black carbon instrument for the measurement of fine light absorbing carbon particles, *Atmospheric Pollution Research*, <https://doi.org/10.1016/j.apr.2021.02.009>].
- [25] B. A. J. Ammerlaan, R. Holzinger, A. D. Jedynsk, J. S. Henzing, (2017). Technical note: Aerosol light absorption measurements with a carbon analyzer Calibration and precision estimates. *Atmospheric Environment*, 164, 1-7.
- [26] Horvath, H., (1993). Atmospheric light absorption – A Review. *Atmospheric Environment* 27, 293-317.
- [27] E. Weingartner, H. Saatho, M. Schnaiter, N. Streit, B. Bitnar, U. Baltensperger. (2003). Absorption of light by soot particles: determination of the absorption coefficient by means of aethalometers. *Aerosol Science* 34, 1445–1463.
- [28] Wu, Y., Yan, P., Tian, P., Tao, J., Li, L., Chen, J., Zhang, Y., Cao, N., Chen, C., Zhang, R., (2015). Spectral light absorption of ambient aerosols in urban Beijing during summer: An intercomparison of measurements from a range of instruments, *Journal of Aerosol Air Quality Research* 15, pp. 1178-1187.
- [29] Mousavi, A.; Sowlat, M. H.; Lovett, C.; Rauber, M.; Szidat, S.; Boffi, R.; Borgini, A.; De Marco, C.; Ruprecht, A. A.; (2019). Sioutas, C. Source apportionment of black carbon (BC) from fossil fuel and biomass burning in metropolitan Milan, Italy. *Atmos. Environ.* 203, 252–261. [CrossRef].
- [30] Kiran, V. R.; Talukdar, S.; Ratnam, M. V.; Jayaraman, A. (2018). Long-term observations of black carbon aerosol over a rural location in southern peninsular India: Role of dynamics and meteorology. *Atmos. Environ.* 189, 264–274. [CrossRef].

- [31] Xiao, S.; Yu, X.; Zhu, B.; Kumar, K. R.; Li, M.; Li, L. (2020). Characterization and source apportionment of black carbon aerosol in the Nanjing Jiangbei New Area based on two years of measurements from Aethalometer. *J. Aerosol Sci.* 139, 105461. [CrossRef].
- [32] Taha, G., Box, G. P., Cohen, D. D., Stelcer, E., (2007). Black carbon measurement using laser integrating plate method, *Journal of Aerosol Science Technology* 41, pp. 266-276.
- [33] Laskin, A., Laskin, J., Nizkorodov, S. A., (2015). Chemistry of atmospheric brown carbon. *Chem. Rev.* 115, 4335–4382.